SPRINGER BRIEFS IN
APPLIED SCIENCES AND TECHNOLOGY

Antonio Luque
Alexander Virgil Mellor

Photon Absorption Models in Nanostructured Semiconductor Solar Cells and Devices

Springer

SpringerBriefs in Applied Sciences and Technology

More information about this series at http://www.springer.com/series/8884

Antonio Luque · Alexander Virgil Mellor

Photon Absorption Models in Nanostructured Semiconductor Solar Cells and Devices

Springer

Antonio Luque
Solar Energy Institute
Polytechnic University of Madrid
Madrid
Spain

and

Nanostructured Solar Cells
Ioffe Physical Technical Institute
St Petersburg
Russia

Alexander Virgil Mellor
Solar Energy Institute
Polytechnic University of Madrid
Madrid
Spain

and

Imperial College of Science
and Technology
London
UK

ISSN 2191-530X ISSN 2191-5318 (electronic)
SpringerBriefs in Applied Sciences and Technology
ISBN 978-3-319-14537-2 ISBN 978-3-319-14538-9 (eBook)
DOI 10.1007/978-3-319-14538-9

Library of Congress Control Number: 2014958579

Springer Cham Heidelberg New York Dordrecht London
© The Author(s) 2015
This work is subject to copyright. All rights are reserved by the Publisher, whether the whole or part of the material is concerned, specifically the rights of translation, reprinting, reuse of illustrations, recitation, broadcasting, reproduction on microfilms or in any other physical way, and transmission or information storage and retrieval, electronic adaptation, computer software, or by similar or dissimilar methodology now known or hereafter developed.
The use of general descriptive names, registered names, trademarks, service marks, etc. in this publication does not imply, even in the absence of a specific statement, that such names are exempt from the relevant protective laws and regulations and therefore free for general use.
The publisher, the authors and the editors are safe to assume that the advice and information in this book are believed to be true and accurate at the date of publication. Neither the publisher nor the authors or the editors give a warranty, express or implied, with respect to the material contained herein or for any errors or omissions that may have been made.

Printed on acid-free paper

Springer International Publishing AG Switzerland is part of Springer Science+Business Media (www.springer.com)

Preface

This book is oriented to optoelectronic device physicists and engineers who want to enter into the realm of quantum calculations for modeling and development of their devices.

As regards quantum mechanics, device physicists generally know their fundamentals and the extent to which they shape the matters of their study; however, given the complexity of the subject matter, time constraints mean that they only become involved in the simplest quantum calculations.

The common background of solid state device physicists and engineers is related to generation and recombination of electron hole pairs and their transport, but in most cases these mechanisms are used in a phenomenological way and no attempt to model the underlying physical mechanism is undertaken. The same can be said about the energy spectrum of the semiconductors used. Contrastingly, balance analyses are frequent in this background.

Among these phenomena, the energy spectrum and mechanism of absorption are considered as properties of the material and their engineering is not considered. With the advent of nanotechnology, this has ceased to be true; the spectrum and the absorption properties can be engineered. Thus they should no longer be treated as a phenomenological input of the device modeling.

Quantum dots (QDs) and quantum wells (QWs) in semiconductors have a typical size range of 2–20 nm compared to atomic unit cells which are 0.5–0.6 nm. In solid state physics, attempts at applying standard quantum mechanical techniques usually require calculation cells with 10,000 atoms or more, which is about the limit of what is feasible even with high-performance computers.

It is the difference between the two characteristic length scales—the mesoscopic nanostructure and the microscopic crystal unit cell—that makes the problem so large. Luckily, within a good approximation, we can decouple the problem into its mesoscopic and microscopic parts. This reduces the complexity of the problem significantly, making it easier to handle both in terms of computation and analysis. Applying the so-called $\mathbf{k}\cdot\mathbf{p}$ techniques to nanostructures serves this purpose; this book is devoted to such techniques.

The mathematical tool more commonly applied by device physicists, due to its simplicity and powerful intuitive content, is the effective mass Schrödinger equation associated to a quantum dot or well. The fundamentals and domain of application are explained in the book. Indeed, the book begins by applying this method to a single effective mass equation with a simple square-potential quantum dot with parallelepiped geometry. Despite its simplicity, the example yields a rich set of consequences, which are studied in detail. Furthermore, this simple example will be a crucial component of the more complex situations to be studied later where several mass equations are used.

The studies in this book are centered on zincblende materials. The highest efficiency solar cells available today are made of these materials as well as most LED diodes. These crystallize in the T_d symmetry group, giving a number of general properties to their respective Hamiltonians, which are thoroughly utilized.

In this book we propose and develop a new k·p Hamiltonian, which we name the Empiric k·p Hamiltonian (EKPH). The EKPH uses four bands: the conduction band (*cb*) and three valence sub-bands: the heavy holes (*hh*), light holes (*lh*) and split-off (*so*) sub-bands. Using the EKPH the full energy spectrum introduced by the quantum nanostructure can be obtained in a few seconds using a laptop. The calculation of the photon absorption coefficients, involving over one thousand transitions, may be obtained in 1.5 hours.

In this book the EKPH is primarily applied to quantum dot and quantum well solar cells. The main validation of the EKPH is the reasonable agreement between the results it produces and those measured in real devices. As further validation, reasonable agreement has also been achieved for the GaAs band-to-band photon absorption. These validations are presented in the book. The accuracy of this fast and simple model is sufficient for many applications in device engineering.

As a comparison, the commonly used eight-band Luttinger-Kohn Hamiltonian, modified by Pikus and Bir for the incorporation of strains induced by the nanostructures, is also presented. This so-called LKPB Hamiltonian is applied using a very simple strain field in order to give the constant band offsets used along this book. Using this method, the time taken for calculation of the quantum efficiency of a quantum dot device is about 170 hours and the results are less accurate with respect to the experimental data than those obtained with the EKPH. Of course, the LKPB Hamiltonian is much more accurate than our EKPH as the proper strain field is adopted. Also, times may be shorter if faster calculation techniques are used. Nonetheless, in all we think that our EKPH Hamiltonian serves as a more useful feedback for the development of better optoelectronic devices than the LKPB Hamiltonian.

Acknowledgments

The authors acknowledge the contribution to this work by many of their colleagues and students at the Institute of Solar Energy (IES) of the Polytechnic University of Madrid (UPM) and of the Ioffe Physical-Technical Institute of St. Petersburg. In particular, the contributions of Professor Antonio Martí, of UPM, and that of the Senior Scientist Alexey Vlasov (who authored Sect. 1.2) and the Ph.D. student Aleksandr Panchak (who made renewed calculations of Fig. 2.8) of Ioffe Institute are acknowledged. Also we acknowledge the role of Professor Viacheslav Andreev in providing one of the authors (AL) a great environment to develop part of this book.

They also acknowledge the support of several funding agencies, some of which are as follows:

- To the Spanish Government by the seminal (1997) SUPERCÉLULA 2FD97-0332-C03-01 project and the GENESIS FV grant CSD2006-0004 of the program CONSOLIDER and the NANOGEFES ENE2009-14481-C02-01 project of the Ministry of Science and Innovation, the last two more directly linked to the work presented here.
- To the Regional Government of Madrid by the NUMANCIA grants S-0505/ENE/0310 and S2009/ENE1477, also directly linked to the work presented here.
- To the European Commission (EC) by the important FULLSPECTRUM SES6-CT-2003-502620 integrated project, the IBPOWER 211640 project and the important NGCPV (283798) EC-Japan Cooperative project.
- To the Russian Government by the important Contract no. 14.B25.31.0020 (Ministry of Education and Science, Resolution 220).

Contents

Chapter 1
Introduction

Abstract This chapter starts with a description of quantum wells and quantum dots. Bandgap tuning using quantum wells is described. It is explained how quantum dots can be used to fabricate an intermediate band solar cell: a third generation concept that should allow the current of a solar cell to be increased without reducing its voltage. A description is given of the state of the art of solar cells containing quantum wells and of intermediate band solar cells made with quantum dots. Quantum well solar cells have been able to produce efficiencies similar to their bulk counterparts, but their tunable bandgaps make then attractive. Present intermediate band solar cells only demonstrate a small increase in generated photocurrent and their voltage is reduced, usually leading to cells that present efficiencies that are lower, or only marginally higher, than single gap counterparts. These issues are examined in this chapter and their origin is described. In all cases, the weak light absorption caused by the quantum structures is a main cause of unsatisfactory performance. This is the main topic of this book: the study of the light absorption by the nanostructures. The chapter ends with a description of the whole book.

Keywords Solar cells · Quantum wells · Quantum dots · Zincblende materials

1.1 Concepts in Nanostructured Solar Cells

Together with many others, nanotechnology has invaded the domain of solar cells. Early proposals [1] included the use of quantum wells (QWs) to adjust the bandgap of the solar cells, and the use quantum dots (QDs) as a means of materializing [2] the intermediate band solar cell (IBSC) [3–5]. Additionally, QDs, often deposited from colloidal solutions, are also widely researched for a variety of solar cell concepts which are beyond the scope of this book. Only semiconductor QDs embedded inside other semiconductors, both with zincblende symmetry (such as InAs in GaAs) are the object of this study.

© The Author(s) 2015

A. Luque and A.V. Mellor, *Photon Absorption Models in Nanostructured Semiconductor Solar Cells and Devices*, SpringerBriefs in Applied Sciences and Technology, DOI 10.1007/978-3-319-14538-9_1

A QW consist of a very thin layer of the QW semiconductor epitaxially grown on the host or barrier semiconductor and covered again by an epitaxial growth of the barrier semiconductor. Usually, the QWs are assembled in arrays. As represented in Fig. 1.1a, the QW solar cell is made by sandwiching a material with QWs between two ordinary semiconductors of n- and p-type respectively. When the QWs are close enough they are sometimes called superlattices.

Other nanostructures are also occasionally used in solar cells with a variety of purposes. We can mention quantum wires formed by long filaments of nanostructure material embedded in the host material, quantum post, or short quantum wires and combinations thereof. These are not further considered in this book.

The adjective quantum refers to that fact that the nanostructure is small enough as to make quantum effects conspicuous. In this respect, the inhomogeneity implied by the QW induces a one-dimensional potential well that leads to eigenfunctions which are the product of three one-dimensional functions each one depending on the variables x, y and z. Taking z as normal to the QW layers, the z-function may be confined within the QW while the x- and y-functions are extended. In contrast, the

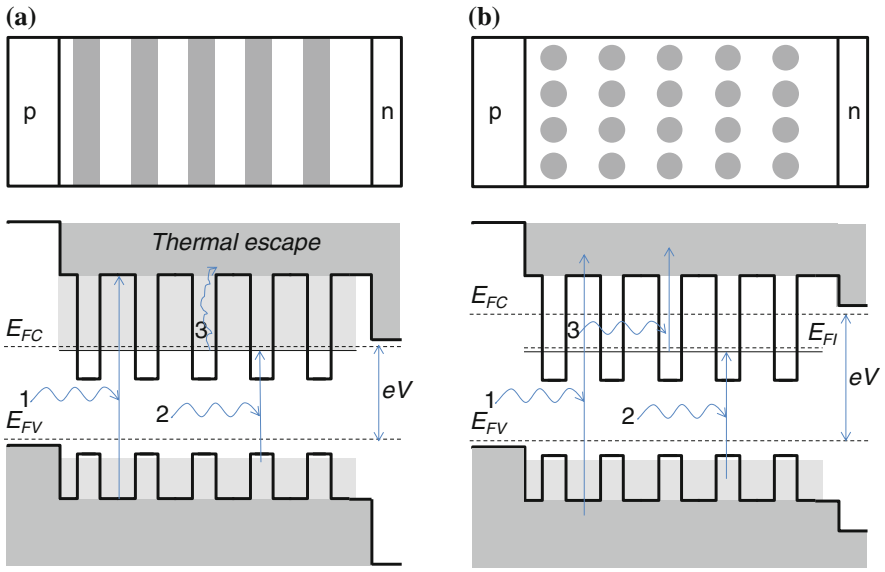

Fig. 1.1 **a** *Above*, the schematic of a QW solar cell and, *below*, its band diagram; besides the pumping of electrons from the VB to the CB by the photons labeled *1*, photons labeled *2* with less energy pump electrons from the VB to the band of QW confined levels. This contributes to the current, since electrons reach the barrier material CB by thermal escape. In this case, the voltage will usually not surpass the bandgap between the VB and the confined levels of the QWs. **b** *Above*, the schematic of a QD solar cell and, *below*, its band diagram. Besides the pumping of electrons from the VB to the CB by absorption of photons labeled *1*, photons labeled *2* with less energy pump electrons from the VB to the IB and photons labeled *3* from the IB to the CB. The voltage can almost reach the CB-VB bandgap. *Grey tones* in the bandgaps represent non-zero density of states: the lighter the lesser

QDs are isolated regions of dot semiconductor inside the barrier semiconductor. These can lead to eigenfunctions that are confined in all dimensions around the QD.

In particular, the potential caused by the QWs is related with the offset of the bands which are well visible in the band diagrams, specifically in that of Fig. 1.1a. As we shall see along the book, the one-dimensional confined wavefunction corresponds to certain discrete energy levels, but because of the extended nature of the other two dimensions, the permitted energies associated to the QW form a continuum that starts in the discrete level and extends upwards as represented in Fig. 1.1a. In the VB, it extends downwards. In the band diagrams in Fig. 1.1 the density of states is (qualitatively) represented by tones of grey, being lighter for lower densities of states. Due to the quantum effects, the energy levels expand inside and outside the QWs.

It is worth noticing that, in the QW, the electron pumped by photon 2 may climb to the CB, where the transport is easy, by absorption of energy from the many phonons and thermal photons available at room temperature. The opposite movement also happens but the thermal equilibrium insures enough density of carriers in the semiconductor CB as to allow for a good transport.

Whereas in the non structured semiconductor the absorption threshold for photons corresponds to the energy of photon 1, in the semiconductor with QWs it corresponds to the energy of photon 2 (in Fig. 1.1a).

The position of the discrete energy level can be regulated by controlling the layer thickness and composition. In this way, these nanostructures are very appropriate to tune the bandgap of the solar cell. This may be useful for multijunction solar cells, where stacks of cells of different bandgaps are used to manufacture very high efficiency solar cells (up to 46 % by autumn 2014).

The IBSC is formed, as represented in Fig. 1.1b, of an intermediate band (IB) material sandwiched between two ordinary semiconductors, one type p and the other type n. In this cell, besides the ordinary pumping with photons 1, electrons may be pumped with photon 2 from the VB to the IB and then with photon 3 from the IB to the CB. In this way two photons of low energy may transport an electron from the VB to the CB, so increasing the cell current. Donors are often added to the QD region to partially fill the IB with electrons and so provide a source for transition 3.

Although the band diagram aspect is almost the same for the QW and the QD solar cell, this is only due to the one dimensional nature of the band diagrams (E-z plots). In reality, the QWs and the QDs have a very different geometrical aspect. The three-dimensional confinement of the QDs leads to isolated energy levels without the continuum of states characteristic of the QWs. In the plot this is represented by the absence of a grey background in the CB potential wells.

Due to the negative effective mass in the VB, the potential pedestals introduced by the nanostructures are equivalent to the wells in the CB. They confine electrons. The reason to draw a light shade for the QDs is that the large effective mass of the heavy holes leads to numerous fully confined states that all together form a quasi-continuum. This means that all the VB states are in strong thermal contact with the extended states of the VB and transitions among them are very frequent causing them to be in thermal equilibrium among themselves.

The voltage of a solar cell is the splitting of the quasi Fermi levels (QFLs) for CB and VB electrons (at their external electrodes, to be precise). In device physics, the electrochemical potentials are called QFLs (E_{FC} and E_{FV} in the drawing). As already said, in QW solar cells there is a relatively large density of states linking the confined-state threshold and the CB. Because of this, all these states are in strong thermal contact with the CB through the interaction with thermal phonons and photons. Therefore, the electrons in these QW states have the same QFL (electrochemical potential) as the CB states. Furthermore, because of the many states, it is very unlikely that this QFL can go much beyond the bottom of the QW threshold of states. Then the voltage is limited to the VB-QW threshold bandgap (see Fig. 1.1a). Contrarily, for the IBSC, there is no continuum of states. Therefore, the IB is (at least ideally) thermally disconnected from the CB. In consequence, the IB has its own QFL (E_{FI}) and nothing prevents the CB and VB QFLs to approach their bands, so permitting a voltage close to the VB-CB bandgap to occur. Because of this the thermodynamic efficiency limit, the IBSC may reach [3] about 63 % versus 41 % for a two-level semiconductor [6], which is what the QW solar cell is.

Unfortunately, this is an ideal situation. Present IBSCs also have some few unwanted states acting as a ladder that thermally connects the IB and the CB, so that the splitting of their QFLs is difficult at room temperature. It is, however, achieved at low temperature and under this condition the cells behave as expected in IBSCs [5].

1.2 Experience with Quantum Well Solar Cells[1]

Research into multi quantum well solar cells (MQW SCs) started in 1990, when Barnham and Duggan suggested the use of QWs for high efficiency solar cells [1]. In general, the main advantage of the MQW SC is that it provides an adjustable bandgap, which is a function of the bandgap widths of the well and barrier materials. The QW area is inserted inside the *i*-region of a *p*-*i*-*n* junction, so that the transport through the structure is facilitated due to a built-in electrical field. For solar PV application, the most popular QW system is based on InGaAs wells placed in the GaAs *p*-*i*-*n* diode. This structure is capable of increasing the short circuit current of the middle GaAs subcell in triple-junction devices. It enables an increase of the monolithic tandem cell efficiency due a better current matching condition.

First QW SCs were strained InGaAs/GaAs structures grown by a team of Imperial College of London (ICL) [7]. It appeared that the strain, gained in such multiple QW structures, limited the number of QWs, due to misfit dislocations during growth, thus limiting the light absorption. Later, it was shown experimentally by a group from the University of Tokyo (UT) [8] that any residual strain

[1] This section is authored by Alexey Vlasov, of the Ioffe Physical Technical Institute, St Petersburg, Russia.

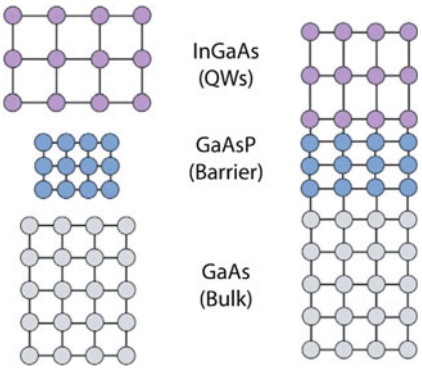

Fig. 1.2 Schematic structure of a strain balanced QW structure. Reprinted with permission. © IOP 2013 [10]

(even a small one) affects the external quantum efficiency (EQE) of the cell. The possible explanation of such behavior is that, in a strained layer, the point defect distribution changes, thus influencing the transport properties of the material.

The approach for the highly efficient solar cells is the use of strain-balanced structures, consisting of InGaAs wells divided by GaAsP barriers (Fig. 1.2). The In and P contents and QW's widths are chosen to minimize the total strain of the system. The first strain-balanced QW cells were also obtained by the ICL team [9, 10]. The cell consisted of 20 MQW's inserted in the GaAs *p-i-n* diode. It was shown that dark I-V curves of the cell were almost unchanged compared to a control GaAs diode, showing an excellent quality of the cell. The EQE spectrum revealed a shoulder in 880–980 nm region with $\sim$20 % efficiency. The I_{SC} value of the QW cell increased a little, although the V_{OC} dropped slightly.

Further attempts were devoted to increasing the QW number for better light absorption. In 2004, Lynch et al. [11] presented a 65 QW SC with an EQE shoulder of 50 % efficiency (which is enough for current matching of the triple GaInP/GaAs-MQW/Ge solar cell) (see Fig. 1.3). At the same time, it was shown that an increase in

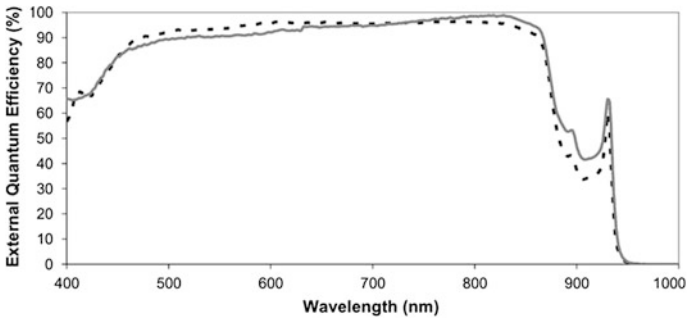

Fig. 1.3 Spectral photoresponse of 50 (*solid line*) and 65 (*dashed line*) MQW solar cells. Reprinted with permission. © Springer 2005 [11]

QW number doesn't necessarily lead to any significant change in V_{OC}, and thus affects mainly the I_{SC} value [12].

The main problem of the MQW SC is the carrier transport, which is realized [13] either by thermal escape from the well (6) or by tunneling through the barrier (5), as shown in Fig. 1.7. The efficiency of these processes is unstable and depends on the electrical field, temperature, light concentration etc. Also, the process of radiative and non-radiative recombination in the QW's (2,3) can reduce the I_{SC} value, affecting the I_{SC} value (Fig. 1.4).

The UT team has indicated the importance of the doping control in the QW SC, a constant value of the electrical field (equal for all wells) should provide better carrier transport through the cell [14]. Also, this team proposed a stepped QW structure for better carrier transport. The QW thus consists of $In_{0.24}Ga_{0.76}As$ wells, $In_{0.13}Ga_{0.87}As$ 1st cladding, GaAs 2nd cladding and GaAsP barriers [15]. The resulting structure revealed better absorption below the GaAs bandgap.

Yet another approach for the strain-balanced QW SC architecture was suggested by the UT team [16]. Normally, the GaAsP barriers contain 10 % phosphorous to keep the barrier bandgap from being too high. In this research the authors introduced superlattices instead of conventional MQW's. In a superlattice, the GaAsP barrier has 43 % phosphorous, which makes it possible to reduce the barrier width down to 3.1 nm, ensuring strain compensation on one hand and good overlapping of wavefunctions on the other. Thus, a band with a lower E_g than that of GaAs is formed. The carrier collection efficiency in such structures did not depend on the electric field. As a result, structures with minimal V_{OC} drop and increased I_{SC} values were presented.

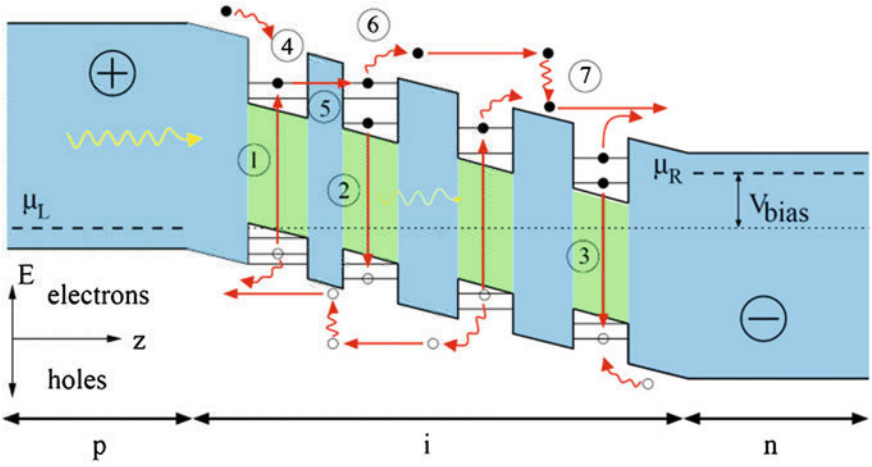

Fig. 1.4 Processes in a MQW SC: *1* Photogeneration of electron-hole pairs. *2* Radiative recombination. *3* Nonradiative recombination (Auger, trap/SRH). *4* Carrier capture. *5* Resonant and non-resonant tunneling. *6* Thermal escape and sweep-out by built in field. *7* Relaxation by inelastic scattering (optical phonons). Reproduced with permission. © SPIE 2010 [13]

Recently the ICL team presented a self-adjusting MQW tandem cell in which both cells (top and bottom) have QW's [17]. In this structure excess carriers in the top InGaAsP/InGaP subcell (e.g. when the blue part of the solar spectrum is enhanced) are captured by the wells and recombine, providing additional radiation for the bottom InGaAs/GaAsP subcell. This process makes the cell less dependent on the solar spectrum, which is very important for terrestrial applications, where the solar spectrum changes hourly and seasonally.

Among other research on MQW SC's, we would like to give attention to the nitrogen based (III-N) system, which has lately become very popular. These materials make use of the potential of the InGaN alloy to overlap the whole solar spectrum (from the 0.65 eV bandgap of InN to the 3.2 eV bandgap of GaN). Also, the reason for so much interest might be the wish to utilize the capability of MOVPE reactors, designed for LED mass-production. The use of QW's in the III-N system seems to be obligatory, due to the strong phase separation of bulk InGaN alloys [18].

1.3 Experience with Intermediate Band Solar Cells

Most of the QD IB solar cell prototypes have been made so far with InAs in a GaAs matrix, grown by molecular beam epitaxy (MBE) in the Stranski-Krastanov mode. The first cell was produced by the Polytechnic University of Madrid in collaboration with the University of Glasgow [19]. However, as is visible in Fig. 1.5, the current increase was negligible and a reduction of voltage was observed, although the contribution of the sub bandgap current is better observed by looking at the quantum efficiency (QE). However this increase is not to be taken straightforwardly as a proof of the IBSC behavior [20].

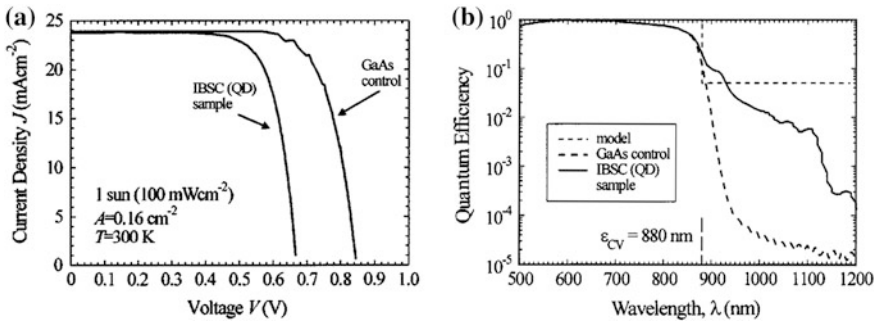

Fig. 1.5 **a** Current-voltage characteristics under one-sun illumination of an IBSC fabricated from InAs QDs and a GaAs control cell. **b** Quantum efficiency of the GaAs control and the QD-IBSC sample. Printed with permission. © 2004, AIP [19]

The deleterious role of the dislocations caused by the growth of the QDs [21] was soon recognized. Actually, the Stranski-Krastanov mode is based on growing a semiconductor of a larger lattice constant (InAs) on one of smaller one (GaAs). The stress is relieved by spontaneous breaking the continuity of the InAs layer, so forming the QDs. However, the structure is still stressed, so resulting in dislocations, which are seriously deleterious for the solar cell operation. Hubbard and coworkers [22] solved this drawback first by insertion thin layers of GaP with a lattice constant still lower than the GaAs, so compensating the effect of the InAs. Actually, they used another growth technique (metal organic chemical vapor deposition-MOCVD) in which the operation with P is easier. The GaP has a larger bandgap too, so that its effect is not visible in the cell operation. Through a very moderate reduction of the voltage and a sensible increase of the current, QD solar cells have been achieved that exceed the efficiency of the test cell of similar characteristics but without QDs [23]. Many other groups have made QD solar cells with slight variations. The best achieved efficiency so far has been 18 %. This was obtained, by a group headed by the Ioffe Institute of St Petersburg [24], through careful cell termination, which is usually neglected by most researchers at this stage of the research.

A strongly simplified IBSC equivalent circuit is given in Fig. 1.6 (inset). It consists of three elementary solar cells linking the VB with the IB, the IB with the CB and a third cell linking the VB and the CB directly. At room temperature, the diode D3 linking the IB and the CB is short circuited by a set of ladder states (to be described later in this book). Consequently, the measured results are characteristic of a cell with the VB-IB bandgap, with less voltage than the reference cell where the bandgap is the VB-CB one. At lower temperatures, the ladder states become less effective and the IBSC voltage converges towards that of the control cell [5, 25, 26]. The voltage of the IBSC cell exceeds that of the reference cell at 20 K (see Fig. 1.6).

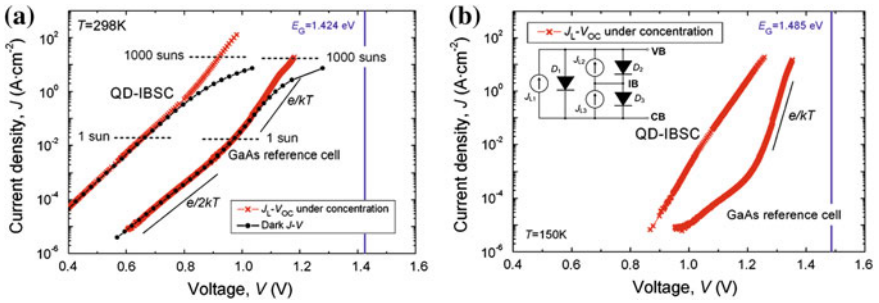

Fig. 1.6 **a** J_{sc}-V_{oc} (*in red*) measured characteristic at several light irradiances of an IBSC and an ordinary reference cell made for comparison at room temperature (**a**) and at 150 K (**b**). At room temperature, the dark current is also drawn (*in black*). Under the superposition principle both *curves* should be the same, but series resistance and other effects make them different. A simplified equivalent circuit is also drawn at the *inset*. Printed with permission. © 2012, Elsevier [25]

Sub bandgap current has been observed although it is too weak. The two photon current associated to the mechanism 2 and 3 of Fig. 1.1b have also been unequivocally observed [27]. The splitting of the Fermi level into three QFLs has also been observed [28]. However, practical IBSCs are not yet available. The optical properties of this structure are a key in understanding the IBSC. This book is devoted to this issue.

1.4 The Zincblende Materials

Most of the III-V semiconductors crystallize in the zincblende structure within the cubic system. This is at least the case for AlP, AlAs, AlSb (with some doubts), GaP, GaAs, GaSb, InP, InAs and InSb, This structure consists of two face-centered cubic lattices, one formed by atoms of the Column IIIA and the other by atoms of the Column VA of the periodic table. Several binary compounds may intermix and form solid solutions that often conserve the same basic structure. We present in Fig. 1.7 the position of the atoms in the zinblende conventional unit cell.

The V type atoms are located in the center of a tetrahedron in whose vertices III atoms are located. This is visible in the figure. The same can be said of the III type atoms, which are also located in the center of a tetrahedron with V atoms at the vertices. Therefore, they have a tetrahedral coordination with four atoms of different nature surrounding each atom. This gives a characteristic band structure with one conduction band and three valence bands, the latter being called the heavy holes, light holes and split off bands. The split off band is at deeper energies in the valence band. This will be seen along this book in closer detail.

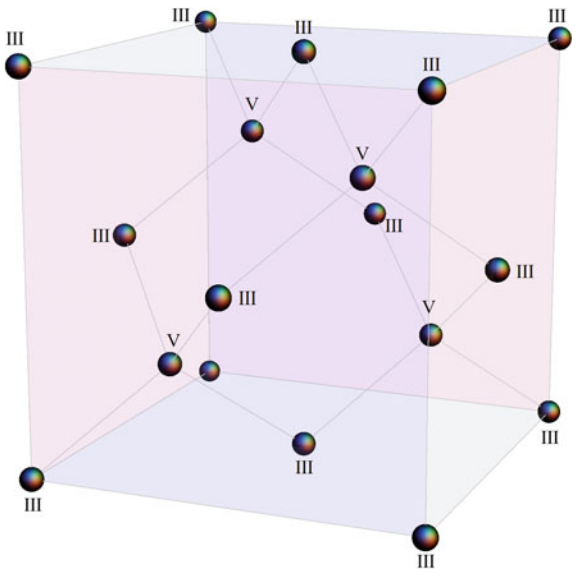

Fig. 1.7 Zincblende lattice. It is formed by two face centered lattices each one displaced by a vector (1/4,1/4,1/4), where the side of the containing cube is taken to be unity. *III* and *V* represent the sites of atoms of the corresponding column